

# Optimal Grid Layouts for Hybrid Offshore Assets in the North Sea under Different Market Designs

Hardy, Stephen  
KU Leuven/EnergyVille

Themelis, Andreas  
Kyushu University

Yamamoto, Kaoru  
Kyushu University

Ergun, Hakan  
KU Leuven/EnergyVille

他

<https://hdl.handle.net/2324/7151987>

---




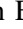
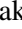
出版情報 : IEEE Transactions on Energy Markets, Policy and Regulation. 1 (4), pp.468-479, 2023-06-26. Institute of Electrical Electronics Engineers (IEEE)

バージョン :

権利関係 :



# Optimal Grid Layouts for Hybrid Offshore Assets in the North Sea under Different Market Designs

Stephen Hardy<sup>1</sup> , Andreas Themelis<sup>2</sup> , Kaoru Yamamoto<sup>2</sup> *Member, IEEE*, , Hakan Ergun<sup>1</sup> *Senior Member, IEEE*,  and Dirk Van Hertem<sup>1</sup> *Senior Member, IEEE*, 

<sup>1</sup>KU Leuven/EnergyVille, Leuven/Genk, Belgium <sup>2</sup>Kyushu University, Fukuoka, Japan

**Abstract**—This work examines the generation and transmission expansion planning problem of offshore grids under different market clearing mechanisms: a home market design, a zonally cleared offshore bidding zone and a nodally cleared offshore bidding zone. It aims at answering two questions. Is knowing the market structure a priori necessary for effective generation and transmission expansion planning? And which market mechanism results in the highest overall social welfare? To this end, a multi-period, stochastic generation and transmission expansion planning formulation is developed for both nodal and zonal market designs. The approach considers the costs and benefits among stakeholders of hybrid offshore assets as well as gross consumer surplus. The methodology is demonstrated on a North Sea test grid based on projects from the European network of transmission system operators' ten-year network development plan. An upper bound on potential social welfare in zonal market designs is calculated and it is concluded that from a generation and transmission perspective, knowing the market structure a priori is not strictly necessary but planning under the assumption of a nodal offshore bidding zone is recommended as it results in the highest overall social welfare and best risk adjusted return.

**Index Terms**—Expansion planning, grid topology, meshed HVDC grids, mixed-integer optimization, offshore wind energy, power generation, power transmission.

## NOMENCLATURE

$\mathcal{A}^{\text{br}}$	Balancing responsible optimization variables
$\mathcal{A}^{\text{te}}$	Transmission expansion optimization variables
$\mathcal{A}_j$	Storage developer optimization variables
$\mathcal{A}_o$	Transmission developer optimization variables
$\mathcal{A}_w$	OWPP developer optimization variables
$\alpha^{\ell, \text{br}}$	Intra-zonal candidate line binary decision variable
$\alpha^{\ell, \text{te}}$	Inter-zonal candidate line binary decision variable
$\alpha^{\ell}$	Candidate line binary decision variable
$P^{\text{j,abs}}$	Set of storage absorption power variables
$P^{\text{j,inj}}$	Set of storage injection power variables
$P^{\text{u}}$	Set of instantaneous demand variables
$\alpha^{\ell}$	Set of candidate transmission line variables
$\theta$	Set of voltage angle variables
$\tilde{P}^{\text{g}}$	Set of candidate generator output variables
$\bar{P}^{\text{g}}$	Set of existing generator output variables
$\hat{S}_{\text{g}}$	Set of candidate generators

$\tilde{S}_{\ell}$	Set of candidate transmission lines
$\theta$	Candidate voltage angle
$\Delta\theta^{\text{max}}$	Maximum voltage angle difference
$\Delta E^{\text{j,max}}$	Change in storage capacity
$\delta I^{\zeta}$	Converter expansion investment
$\delta I^{\text{g}}$	Generation expansion investment
$\delta I^{\text{j}}$	Storage expansion investment
$\Delta P^{\text{g,max}}$	Change in generation capacity
$\Delta P^{\zeta, \text{max}}$	Change in converter capacity
$\Delta E^{\text{j,max}}$	Set of change in max storage capacity variables
$\Delta P^{\zeta, \text{max}}$	Set of change in max converter capacity variables
$\Delta \tilde{P}^{\text{g,max}}$	Set of change in max generator capacity variables
$\mathcal{E}$	Set of all (directed) edges
$\mathcal{E}^{\text{AC}}$	Set of AC network edges
$\mathcal{E}^{\text{DC}}$	Set of DC network edges
$\mathcal{E}^{\text{br}}$	Set of intra-zonal edges
$\mathcal{E}^{\text{te}}$	Set of inter-zonal edges
$\mathcal{E}^{\text{AC-DC}}$	Set of all edges between AC and DC networks
$\eta^{\text{j,abs}}$	Charge efficiency of storage
$\eta^{\text{j,inj}}$	Discharge efficiency of storage
$\hat{S}_{\text{g}}$	Set of existing generators
$\hat{S}_{\ell}$	Set of existing transmission lines
$\gamma^{\text{j}}$	Self-discharge rate
$\lambda$	Market clearing price
$\mathcal{N}$	Set of all nodes
$\mathcal{N}^{\text{AC}}$	Set of all AC nodes
$\mathcal{N}^{\text{DC}}$	Set of all DC nodes
$\pi_s$	Probability of scenario $s$
$\Psi^{\text{g}}$	RES generator time series
$\Psi^{\text{u}}$	Demand time series
$S_{\text{g}}$	Set of all generators
$S_{\text{j}}$	Set of storage devices
$S_{\ell}$	Set of all transmission lines
$S_{\text{s}}$	Set of scenarios
$S_{\text{t}}$	Set of hours
$S_{\text{u}}$	Set of demands
$S_{\text{y}}$	Set of years
$\tau$	Transformer ratio
$\theta$	Voltage angle
$\theta^{\text{max}}$	Maximum voltage angle
$\theta^{\text{min}}$	Minimum voltage angle
$\widehat{E^{\text{j,max}}}$	Maximum expansion capacity of candidate storage
$\widehat{P^{\text{g,max}}}$	Maximum expansion capacity of candidate generators
$\widehat{P^{\zeta, \text{max}}}$	Maximum expansion capacity of candidate converters
$\xi^{\text{j,c}}$	Maximum charge rate

This project has received funding from the CORDOBA project funded by Flanders Innovation and Entrepreneurship (VLAIO) in the framework of the spearhead cluster for blue growth in Flanders (Blue Cluster) – Grant number HBC.2020.2722, and from the Japan Society for the Promotion of Science (JSPS) KAKENHI grants no. JP19H02161, JP20K14766 and JP21K17710. A special thanks to Michiel Kenis and Prof. Jef Berten for their input regarding energy market modelling. ChatGPT [1] has been consulted for checking grammar and improving sentence structure.

$\xi^{j,d}$	Maximum discharge rate
$\mathcal{Z}$	Set of market zones
$b$	Transmission line susceptance
$C^g$	Generator bid price
$C^u$	Consumer bid price
$E^{j,\max}$	Maximum capacity of candidate storage
$E^j$	Capacity of candidate storage
$f^H$	NPV scalar for hourly revenues
$f^Y$	NPV scalar for yearly revenues
$I^\ell$	Candidate line investment
$L^\zeta$	Converter loss factor
$P^{\ell,\max}$	Maximum transmission line power
$P^\ell$	Instantaneous Transmission line power
$P^{g,\max}$	Maximum generator power
$P^g$	Instantaneous generator power
$P^{j,abs}$	Instantaneous storage charging power
$P^{j,inj}$	Instantaneous storage discharging power
$P^{u,\max}$	Maximum demand power
$P^u$	Instantaneous demand power
$P^{\zeta,\max}$	Maximum converter power
$P^{\zeta,AC}$	Instantaneous AC side converter power
$P^{\zeta,DC}$	Instantaneous DC side converter power
$P^{\zeta,loss}$	Instantaneous converter power losses
$T$	Hours per simulation year

## I. INTRODUCTION

### A. Motivation

Recent events in Europe and around the world have created an environment where a rapid transition of the energy supply towards a safe, secure and carbon neutral system is essential. The issues of climate change have converged with an urgent need to reduce the dependence on Russian gas in light of the invasion of Ukraine. In response to the invasion, the European Commission recently presented the 300 B€ RE-powerEU plan to rapidly scale-up Renewable Energy Sources (RESs) and network electrification. The plan builds on the already ambitious targets under the Fit for 55 plan, increasing renewable generation targets from 1067 GW to 1236 GW by 2030 [2].

Offshore wind in the North Sea is crucial in meeting these targets. The North Sea governments of Belgium, Denmark, the Netherlands and Germany have pledged to increase the installed capacity of North Sea offshore wind farms to 65 GW by 2030 and to 150 GW by 2050 [3]. This is a substantial step towards the EU wide goal of 240 to 450 GW of offshore wind by 2050, which is needed to meet the climate targets agreed upon under The Paris Agreement [4], [5].

In addition to expanding offshore wind, investments in transmission infrastructure are required. To this end, the European Network of Transmission System Operators for Electricity (ENTSO-E) releases a Ten Year Network Development Plan (TYNDP) every two years to identify essential infrastructure investments [6]. To date, 43 offshore transmission projects, including interconnectors, Hybrid Offshore Assets (HOAs) and Offshore Wind Power Plant (OWPP) connections, totalling 65.6 GW of capacity, are set to be commissioned by 2035. The number of projects is set to increase further as according to EU regulation 2022/869, article 14, by 2024 the

TYNDP must include a high level infrastructure investment plan for each of the sea-basins under development [7].

To ensure such investments in infrastructure result in efficient use of resources and effective incentives for developers, a carefully designed offshore electricity market that can meet both short-term operational requirements and the needs of long-term investments is required.

### B. Background

*Long-term planning:* Much research into regulatory, technological and economic aspects of a North Sea grid has been performed [8]–[10]. There is a consensus that such a grid would be a meshed High Voltage Direct Current (HVDC) grid. The economic and technical advantages of choosing HVDC are summarized in [11] while some of the technical challenges can be found in [12].

The Generation and Transmission Expansion (GATE) planning problem aims at determining the least cost power system design and in its complete form is a Mixed Integer NonLinear Program (MINLP) [13]. Due to the difficulty of solving such a problem, the reactive power component of the nonlinear power flow equations is often ignored and a linear “DC” power flow [14] or convex relaxation such as in [15]–[17] is assumed.

In its most common form the problem takes a central planner’s perspective as in [18], [19]. Another common way to formulate it is as an equilibrium model such as [20], [21]. The problem can be formulated as a static (single time step) [20], [22] or dynamic (multi-step) problem [23]. Uncertainty is often handled using stochastic programming as in [24]–[26] or robust optimization as in [27]–[29]. When analyzing energy markets, multi-level programming such as in [30], [31] has been used.

With market-aware expansion planning formulations, tractability is a serious concern as they are multi-level programs, making a compromise as to what is included in the model a necessity. One of the most common simplifications is to consider either only generation expansion as in [19]–[23], [26] or only transmission expansion as in [28], [29], [31]. It is also possible to consider both in unison and ignore the market as in [24]. Considering all aspects together is quite difficult and requires a multi-level methodology. This is often only demonstrated on toy problems such as in [30], which presents a maximum test size of 6 buses with 2 candidate transmission lines and 3 candidate generators. In [18], a realistic test case is managed but it is still small, limiting the number of candidate lines to 5 and candidate generators to 3. The computation time for this problem is reported as 12.25 hours. As the problem considered in this work is much larger, with several thousand candidate transmission lines and half a dozen candidate generators, a different approach had to be sought.

Furthermore, although the state of the art approaches provide good insight into expansion planning under uncertainty within a pre-determined market structure, they do not assist in deciding on the market structure when it is unknown a priori. Unfortunately, it is within this literature gap that we find ourselves today, moving towards a meshed offshore HVDC grid

without a clearly defined energy market structure for developers to reliably predict future revenues [32].

This high level of uncertainty for developers translates directly to higher costs of development. In this work we aim at filling this gap by providing a method of quantifying the impact different energy market structures have on the GATE planning problem, providing much needed insight towards establishing regulatory clarity.

**Energy Markets:** In liberalized energy markets both nodal and zonal market structures can be found. Examples of the former can be found in North America while in Europe a zonal based system is the norm. For further details on market design, we refer the readers to [32], [33].

A topic currently under debate is the structure of the energy market for an offshore grid and in particular HOAs [32]. HOAs yield benefits for both OWPPs and grid expansion in unison, combining transmission, generation and storage into a single asset. For individual stakeholders, however, there is high uncertainty in expected profitability based on market design and regulation. Currently, there are three market designs under serious consideration, the Home Market Design (HMD), the zonal Offshore Bidding Zone (zOBZ) and the nodal Offshore Bidding Zone (nOBZ) [34]. In an HMD, HOAs are considered part of the energy market of the Exclusive Economic Zone (EEZ) within which they are situated. In a zOBZ, multiple or all HOAs are grouped into a common offshore market zone with a single market price. In an nOBZ all HOAs are in independent market zones, permitting fully localized energy pricing based on inter-nodal congestion.

**Contributions and paper structure:** In this work a multi-period, stochastic, Mixed Integer Linear Program (MILP) is developed. The main contributions of this work are:

- A modelling formulation for different market structures within the GATE planning problem.
- A measurement of the upper bound on social welfare when considering a zonal market design.
- A cost-benefit analysis of a North Sea test case comparing an HMD, an nOBZ and a zOBZ.

In the next section a brief discussion on nodal and zonal markets is presented. Following this, the modelling methodology is described. This begins with the nodal market model in §III-A and is followed in §III-B by the zonal market model. In §IV the North Sea test grid is described along with the modelling assumptions. In §V the results are presented. Finally, in §VI, conclusions and recommendations based on the modelling results round out the paper.

## II. NODAL VERSUS ZONAL MARKETS

In the interest of transparency, the authors of this study declare a pre-existing bias towards nodal pricing due to the price signals in regards to network inefficiencies such as congestion and under supply. These signals can be suppressed in a zonal system and are of very high value, especially at a time of such anticipated network expansion. It is opinioned that localized pricing should be the default and any deviation should be done with caution and only when supported by strong evidence.

Despite the known benefits of nodal pricing, it is possible to find examples where zonal pricing results in an arguably better

outcome for consumers. In studying such examples we hope to meaningfully contribute to the ongoing debate regarding North Sea market structure. To illustrate this point we present a simplified market clearing example involving a pivotal supplier. The assumed market structure is a day-ahead pay-as-cleared (uniform pricing method) market [35] with imbalances settled via an idealized Regulatory re-Dispatch with Cost Compensation (RDCC) [36]. Market participants are assumed to bid truthfully at their marginal price of production.

In the pivotal supplier scenario, we have a topology similar to that of Fig. 1. At node  $m$ , 5 MW of wind generation is present. At node  $n$ , 5 MW of PV, 5 MW of thermal generation and 10 MW of demand are present. A transmission line with a maximum capacity of 4 MW connects nodes  $m$  and  $n$ . Assumed marginal generation costs for RESs and thermal generation are 10 €/MWh and 100 €/MWh respectively.

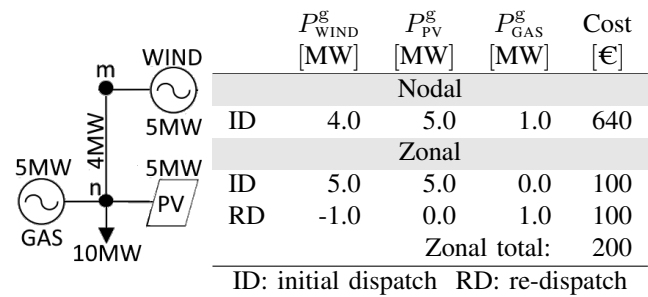


Figure 1: Single line diagram of simple market clearing topology (left). Dispatch and re-dispatch amounts and costs in nodal and zonal market clearing mechanisms (right).

In the nodal market clearing model the 4 MW capacity limit between node  $m$  and  $n$  is considered from the start, resulting in an optimal dispatch of 4 MW of wind at node  $m$ , 5 MW of PV at node  $n$  and 1 MW of thermal at node  $n$ . The resulting clearing prices are 10 €/MWh at node  $m$  and 100 €/MWh at node  $n$ . The total cost of supplying the load is 640 €.

Contrasting this with the zonal clearing model, the line congestion between  $m$  and  $n$  is initially ignored resulting in an optimal dispatch of 5 MW of wind at node  $m$  and 5 MW of PV at node  $n$  with a zonal clearing price of 10 €/MWh. The cost prior to re-dispatch is therefore 100 €. As the capacity constraint from node  $m$  to  $n$  is violated, however, the balancing authority directs the down regulation of wind to 4 MW at node  $m$  and up regulation of the thermal plant at node  $n$  to 1 MW. The balancing responsible pays a total re-dispatch cost of 100 € to the thermal plant and the total cost to supply the load is 200 € (assuming no avoided variable costs for the OWPP).

This is arguably a more desirable result for consumers. Of course, in the case of the pivotal supplier it can be correctly argued that the efficiency of the market is creating a high clearing price to signal that either additional transmission from  $m$  to  $n$  or additional generation at node  $n$  is needed. However, in a grid with a high penetration of highly fluctuating sources, it may be an unusually low wind or solar irradiation day that transforms a certain generator into a pivotal supplier. The question as to whether an investment to increase trans-

mission or generation is warranted is more complicated, as it depends on the frequency with which the pivotal supplier negatively impacts energy prices. In this case, a cost-benefit analysis should be performed, ensuring sufficient infrastructure investment is made to effectively and economically meet demand while guaranteeing long term stability.

### III. PLANNING MODEL

The developed model is based on one first presented in [37] with the principle additions being the consideration of benefits, rather than costs alone, the ability to expand generation and the inclusion of multiple market structures. The Gurobi solver version 0.9.14 [38] is used when solving the MILP.

Special notation:

- $x : n$  ( $x$  located at node  $n$ ).
- $x : mn$  ( $x$  located on directed edge  $mn$ ).
- $x : \{mn\}$  ( $x$  located on undirected edge  $mn$ ).

#### A. Nodal Market Model

1) *Objective Function:* An existing network operator ( $\mathcal{A}_e$ ) and a set of developers of OWPPs ( $\mathcal{A}_w$ ), offshore transmission ( $\mathcal{A}_o$ ) and storage ( $\mathcal{A}_j$ ) have costs and benefits associated with their operation and development as defined in (1) – (4). The costs and benefits are divided into two distinct parts: hourly operational costs and benefits and yearly strategic investments. The Net Present Value (NPV) equivalents of hourly and yearly revenue and expenditure streams are determined by scalars  $f_y^H$  and  $f_y^Y$  respectively. A discount rate of 4% is assumed.

An OWPP developer ( $\mathcal{A}_w$ ) can make a strategic yearly investment to expand the capacity of an OWPP ( $\Delta P_{\tilde{g}}^{\max}$ ) as in (1a). Hourly benefits can then be accrued by selling the energy generated on the spot market at a price  $\lambda_n$ . The marginal cost of production is assumed to be zero.

$$\mathcal{U}_{y,s}^w = -f_y^Y \left[ (1a) \right] \quad (1)$$

$$\sum_{n \in \mathcal{N}^{AC}} \sum_{\tilde{g} \in \tilde{\mathcal{S}}_{g:n}} \delta I_{\tilde{g}:n,y}^g \cdot \Delta P_{\tilde{g}:n,y}^{g,\max} \quad (1a)$$

An offshore transmission developer ( $\mathcal{A}_o$ ) can make a strategic yearly investment to build new transmission lines ( $\alpha_{\tilde{t}}^{\ell}$ ) as in (2a) and/or expand HVDC converter capacity ( $\Delta P_{ne}^{\zeta,\max}$ ) as in (2b). Hourly benefits are then accrued through spatial arbitrage of price differentials ( $\lambda_m - \lambda_n$ ) located in different energy markets. This is also known as congestion rent.

$$\mathcal{U}_{y,s}^o = -f_y^Y \left[ (2a) + (2b) \right] \quad (2)$$

$$\sum_{\substack{\{mn\} \subseteq \mathcal{N} \\ mn \in \mathcal{E}}} \sum_{\tilde{t} \in \tilde{\mathcal{S}}_{\ell:\{mn\}}} \alpha_{\tilde{t}:\{mn\},y}^{\ell} \cdot I_{\tilde{t}:\{mn\},y}^{\ell} \quad (2a)$$

$$\sum_{ne \in \mathcal{E}^{AC-DC}} \delta I_{ne,y}^{\zeta} \cdot \Delta P_{ne,y}^{\zeta,\max} \quad (2b)$$

A storage developer ( $\mathcal{A}_j$ ) can make a strategic yearly investment to expand storage capacity ( $\Delta E_j^{j,\max}$ ) as in (3a). Hourly benefits are then accrued through temporal arbitrage of price

differentials ( $\lambda_{n,t} - \lambda_{n,t+\Delta t}$ ). The marginal cost of charging and discharging is assumed to be zero.

$$\mathcal{U}_{y,s}^j = -f_y^Y \left[ (3a) \right] \quad (3)$$

$$\sum_{n \in \mathcal{N}} \sum_{j \in \mathcal{S}_{j:n}} \delta I_{j:n,y}^j \cdot \Delta E_{j:n,y}^{j,\max} \quad (3a)$$

The existing network operator has hourly costs and benefits associated with existing generation (4a) and consumption (4b). Existing generators accrue hourly benefits through the sale of energy ( $P_{\tilde{g}}^g$ ) on the spot market at a price ( $\lambda_n$ ) higher than their marginal production cost ( $C_{\tilde{g}}^g$ ). Consumers benefit when the price of energy  $\lambda_n$  is lower than the consumer's bid price ( $C_u^u$ ) resulting in a surplus.

$$\mathcal{U}_{y,s}^e = f_y^H \sum_{t \in \mathcal{S}_t} \left[ (4a) + (4b) \right] \quad (4)$$

$$\sum_{n \in \mathcal{N}^{AC}} \sum_{\tilde{g} \in \tilde{\mathcal{S}}_{g:n}} (-C_{\tilde{g}:n,t,y,s}^g) \cdot P_{\tilde{g}:n,t,y,s}^g \quad (4a)$$

$$\sum_{n \in \mathcal{N}^{AC}} \sum_{u \in \mathcal{S}_{u:n}} C_{u:n,t,y,s}^u \cdot P_{u:n,t,y,s}^u \quad (4b)$$

Combining (1)–(4) gives the global objective executed by an all knowing centralized authority to maximize the social welfare of the system ( $\mathcal{U}$ ), as in (5). Social welfare is therefore defined as the sum over all scenarios  $\mathcal{S}_s$  of Gross Consumer Surplus (GCS) and net developer benefits. The final distribution of developer benefits and the GCS is calculated based on the resultant market clearing prices  $\lambda_n$ . The uncertainty of long term planning is captured by the probability  $\pi_s$  of occurrence of a given scenario. Multi-period planning is performed over the lifetime considering the years defined in set  $\mathcal{S}_y$ .

$$\max_{\mathcal{A}_w, \mathcal{A}_o, \mathcal{A}_j, \mathcal{A}_e} \mathcal{U} := \sum_{s \in \mathcal{S}_s} \pi_s \sum_{y \in \mathcal{S}_y} \mathcal{U}_{y,s}^w + \mathcal{U}_{y,s}^o + \mathcal{U}_{y,s}^j + \mathcal{U}_{y,s}^e \quad (5)$$

where

$$\mathcal{A}_w = (\tilde{P}^g, \Delta \tilde{P}^{g,\max}), \quad \mathcal{A}_o = (\theta, \alpha^{\ell}, \Delta P^{\zeta,\max}),$$

$$\mathcal{A}_j = (P^{j,\text{inj}}, P^{j,\text{abs}}, \Delta E^{j,\max}), \quad \mathcal{A}_e = (\bar{P}^g, P^u)$$

2) *Constraints:* Generation consisting of both RESs and conventional generation must remain within capacity limits. This is ensured by constraint (6). For RESs, parameter  $\Psi_{\tilde{g}}^g$  is the per-unit RES generation time series and for conventional generators it is equal to one.

$$0 \leq P_{\tilde{g}:n,t,y,s}^g \leq \Psi_{\tilde{g}:n,t,y,s}^g \cdot P_{\tilde{g}:n,y}^{g,\max} \quad (6)$$

$$n \in \mathcal{N}^{AC}, \quad g \in \mathcal{S}_{g:n}, \quad t \in \mathcal{S}_t, \quad y \in \mathcal{S}_y, \quad s \in \mathcal{S}_s$$

In the particular case that the generator is a candidate OWPP under consideration for expansion,  $P_{\tilde{g}}^{g,\max}$  is constrained from above by  $\widehat{P_{\tilde{g}}^{g,\max}}$  and may only increase or remain constant year over year as in:

$$P_{\tilde{g}:n,y}^{g,\max} \leq \widehat{P_{\tilde{g}:n,y}^{g,\max}}, \quad P_{\tilde{g}:n,y-\Delta y}^{g,\max} \leq P_{\tilde{g}:n,y}^{g,\max} \quad (7)$$

$$\tilde{g} \in \tilde{\mathcal{S}}_{g:n}, \quad n \in \mathcal{N}^{AC}, \quad y \in \mathcal{S}_y,$$

where  $\Delta y$  is the number of years between modelling years.  $P_{\tilde{g}:n,y-\Delta y}^{g,\max}$  in the first year is assumed to be zero. Demand is

set via time series  $\Psi_u^u$  as in (8). A high cost for load shedding ensures it is only a last resort.

$$0 \leq P_{u:n,t,y,s}^u \leq \Psi_{u:n,t,y,s}^u \quad (8)$$

$$n \in \mathcal{N}^{\text{AC}}, \quad u \in \mathcal{S}_{u:n}, \quad t \in \mathcal{S}_t, \quad y \in \mathcal{S}_y, \quad s \in \mathcal{S}_s$$

A storage device has a state of charge  $E_j^j$  at each time step  $\Delta t$  defined by the following constraint:

$$E_{j:n,t,y,s}^j = (1 - \gamma_{j:n}^j) \Delta t E_{j:n,t-\Delta t,y,s}^j + \Delta t (\eta_{j:n}^{\text{abs}} P_{j:n,t,y,s}^{\text{abs}} - \frac{P_{j:n,t,y,s}^{\text{inj}}}{\eta_{j:n}^{\text{inj}}}) \quad (9)$$

$$j \in \mathcal{S}_{j:n}, \quad n \in \mathcal{N}^{\text{AC}}, \quad t \in \mathcal{S}_t^*, \quad y \in \mathcal{S}_y, \quad s \in \mathcal{S}_s,$$

where  $\mathcal{S}_t^*$  denotes the set of all time steps except the first one. Here,  $\gamma_j^j$  is the self discharge rate and  $\eta_j^{\text{abs}}$  and  $\eta_j^{\text{inj}}$  are the charge and discharge efficiencies respectively.

The current state of charge is constrained between zero and the rating of the device  $E_j^{\text{j,max}}$ . The device rating can be expanded up to a maximum of  $\widehat{E_j^{\text{j,max}}}$  but may only increase or remain constant year over year as in:

$$0 \leq E_{j:n,t,y,s}^j \leq E_{j:n,y}^{\text{j,max}} \quad \left. \begin{array}{l} n \in \mathcal{N}^{\text{AC}}, j \in \mathcal{S}_{j:n} \\ t \in \mathcal{S}_t, y \in \mathcal{S}_y \\ s \in \mathcal{S}_s \end{array} \right\} \quad (10)$$

$$E_{j:n,y-\Delta y}^{\text{j,max}} \leq E_{j:n,y}^{\text{j,max}} \leq \widehat{E_{j:n,y}^{\text{j,max}}}$$

In the first year,  $E_{j:n,y-\Delta y}$  is assumed to be zero. A storage device has a maximum rate at which it can charge and discharge, this is ensured by (11).  $\xi_j^{\text{j,c}}$  and  $\xi_j^{\text{j,d}}$  are the normalized charge and discharge rates.

$$0 \leq P_{j:n,t,y,s}^{\text{j,abs}} \leq \xi_{j:n}^{\text{j,c}} \cdot E_{j:n,y}^{\text{j,max}} \quad \left. \begin{array}{l} n \in \mathcal{N}^{\text{AC}}, j \in \mathcal{S}_{j:n} \\ t \in \mathcal{S}_t, y \in \mathcal{S}_y \\ s \in \mathcal{S}_s \end{array} \right\} \quad (11)$$

$$0 \leq P_{j:n,t,y,s}^{\text{j,inj}} \leq \xi_{j:n}^{\text{j,d}} \cdot E_{j:n,y}^{\text{j,max}}$$

Constraint (12) sets the initial and final states of charge in each year to half capacity. The final constraint on storage, to not simultaneously charge and discharge is not explicitly enforced, rather, it is implicitly guaranteed via charge and discharge efficiencies less than one.

$$E_{j:n,1,y,s}^j = \frac{E_{j:n,y}^{\text{j,max}}}{2} + \eta_{j:n}^{\text{abs}} P_{j:n,1,y,s}^{\text{abs}} - \frac{P_{j:n,1,y,s}^{\text{inj}}}{\eta_{j:n}^{\text{inj}}} \quad \left. \begin{array}{l} n \in \mathcal{N}^{\text{AC}} \\ j \in \mathcal{S}_{j:n} \\ y \in \mathcal{S}_y \\ s \in \mathcal{S}_s \end{array} \right\} \quad (12)$$

$$E_{j:n,T,y,s}^j = \frac{E_{j:n,y}^{\text{j,max}}}{2}$$

The AC and DC network constraints described below are implemented using the PowerModels(ACDC).jl packages [39], [40]. A bus injection model is used for AC network branches while considering the linear DC power flow approximations as in (13). Transformers are lumped into the branch model via the transformation ratio  $\tau$ , which is unity when no transformer is required.

$$P_{l:mn,t,y,s}^{\ell} = \frac{b_{l:\{mn\}}}{\tau} [\theta_{m,t,y,s} - \theta_{n,t,y,s}] \quad (13)$$

$$P_{l:mn,t,y,s}^{\ell} = \frac{b_{l:\{mn\}}}{\tau} [\tilde{\theta}_{l:mn,t,y,s} - \tilde{\theta}_{l:nm,t,y,s}]$$

$$|P_{l:mn,t,y,s}^{\ell}| \leq P_{l:\{mn\}}^{\ell,\text{max}} \quad (14)$$

$$|P_{l:mn,t,y,s}^{\ell}| \leq P_{l:\{mn\}}^{\ell,\text{max}} \cdot \alpha_{l:\{mn\},y}^{\ell}$$

$$mn \in \mathcal{E}^{\text{AC}}, \quad \bar{l} \in \bar{\mathcal{S}}_{l:\{mn\}}^{\text{AC}}, \quad \tilde{l} \in \tilde{\mathcal{S}}_{l:\{mn\}}^{\text{AC}}$$

$$t \in \mathcal{S}_t, \quad y \in \mathcal{S}_y, \quad s \in \mathcal{S}_s$$

Power flow through any branch must respect the branch limits as in (14). Nodal voltage angle limits and the maximum divergence between connected nodes are constrained by (15).

$$\theta^{\min} \leq \theta_{n,t,y,s} \leq \theta^{\max} \quad \left. \begin{array}{l} mn \in \mathcal{E}^{\text{AC}} \\ \tilde{l} \in \tilde{\mathcal{S}}_{l:\{mn\}}^{\text{AC}} \\ t \in \mathcal{S}_t \\ y \in \mathcal{S}_y \\ s \in \mathcal{S}_s \end{array} \right\} \quad (15)$$

$$|\theta_{n,t,y,s} - \theta_{m,t,y,s}| \leq \Delta \theta^{\text{max}}$$

$$\theta^{\min} \leq \tilde{\theta}_{l:mn,t,y,s} \leq \theta^{\max}$$

$$|\tilde{\theta}_{l:mn,t,y,s} - \tilde{\theta}_{l:nm,t,y,s}| \leq \Delta \theta^{\text{max}}$$

$$|\tilde{\theta}_{l:mn,t,y,s} - \theta_{m,t,y,s}| \leq (1 - \alpha_{l:\{mn\},y}^{\ell}) \cdot M$$

The final constraint in (15) is only necessary when candidate branches are considered. This constraint leaves candidate line angles unconstrained when the branch is not included, i.e.  $\alpha^{\ell} = 0$ , while enforcing equality with the existing voltage angle when the branch is active, i.e.  $\alpha^{\ell} = 1$ . The AC network is linked to the DC network via an HVDC converter with a maximum AC side capacity of  $P_{ne,y}^{\zeta,\text{max}}$ .  $P_{ne,y}^{\zeta,\text{max}}$  is constrained from above by  $\widehat{P_{ne,y}^{\zeta,\text{max}}}$  and can only increase or remain constant year over year as in:

$$|P_{ne,t,y,s}^{\zeta,\text{AC}}| \leq P_{ne,y}^{\zeta,\text{max}} \quad \left. \begin{array}{l} ne \in \mathcal{E}^{\text{AC-DC}} \\ t \in \mathcal{S}_t \\ y \in \mathcal{S}_y \\ s \in \mathcal{S}_s \end{array} \right\} \quad (16)$$

$$P_{ne,y-\Delta y}^{\zeta,\text{max}} \leq P_{ne,y}^{\zeta,\text{max}} \leq \widehat{P_{ne,y}^{\zeta,\text{max}}}$$

The AC side power is linked to the DC side power through the non negative converter losses:  $L^{\zeta}$ . This, and the upper limit on DC side power is set by:

$$P_{en,t,y,s}^{\zeta,\text{DC}} \leq (1 - L^{\zeta}) P_{ne,y}^{\zeta,\text{max}} \quad \left. \begin{array}{l} ne \in \mathcal{E}^{\text{AC-DC}} \\ t \in \mathcal{S}_t \\ y \in \mathcal{S}_y \\ s \in \mathcal{S}_s \end{array} \right\} \quad (17)$$

$$(L^{\zeta} - 1) P_{ne,y}^{\zeta,\text{max}} \leq P_{en,t,y,s}^{\zeta,\text{DC}}$$

$$P_{ne,t,y,s}^{\zeta,\text{loss}} = L^{\zeta} P_{ne,t,y,s}^{\zeta,\text{AC}} \geq 0$$

$$P_{ne,t,y,s}^{\zeta,\text{AC}} + P_{en,t,y,s}^{\zeta,\text{DC}} = P_{ne,t,y,s}^{\zeta,\text{loss}}$$

In the DC network, linearized power flow reduces to a network flow model (18). DC side power flow through transmission lines must remain within limits as in (19).

$$P_{l:ef,t,y,s}^{\ell} = -P_{l:fe,t,y,s}^{\ell} \quad (18)$$

$$P_{l:ef,t,y,s}^{\ell} = -P_{l:fe,t,y,s}^{\ell}$$

$$|P_{l:ef,t,y,s}^{\ell}| \leq P_{l:\{ef\}}^{\ell,\text{max}} \quad (19)$$

$$|P_{l:ef,t,y,s}^{\ell}| \leq P_{l:\{ef\}}^{\ell,\text{max}} \cdot \alpha_{l:\{ef\},y}^{\ell}$$

$$ef \in \mathcal{E}^{\text{DC}}, \quad \bar{l} \in \bar{\mathcal{S}}_{l:\{ef\}}^{\text{DC}}, \quad \tilde{l} \in \tilde{\mathcal{S}}_{l:\{ef\}}^{\text{DC}}$$

$$t \in \mathcal{S}_t, \quad y \in \mathcal{S}_y, \quad s \in \mathcal{S}_s$$

Finally, Kirchhoff's current law must be satisfied for both AC and DC grids. On the AC side the nodal power balance is given by (20). The AC nodal balance equation is a complicating constraint that links the optimization variables. The dual variable of the constraint is  $\lambda_m$ , the marginal price of energy.

$$\sum_{e \in \mathcal{N}_m^{\text{DC}}} P_{me,t,y,s}^{\zeta,\text{AC}} - \sum_{n \in \mathcal{N}_m^{\text{AC}}} \sum_{l \in \mathcal{S}_{l:\{mn\}}^{\text{AC}}} P_{l:mn,t,y,s}^{\ell} \quad \left. \begin{array}{l} m \in \mathcal{N}^{\text{AC}} \\ t \in \mathcal{S}_t \\ y \in \mathcal{S}_y \\ s \in \mathcal{S}_s \end{array} \right\} \quad (20)$$

$$+ \sum_{g \in \mathcal{S}_{g:n}} P_{gm,t,y,s}^{\text{g}} - \sum_{u \in \mathcal{S}_{u:n}} P_{um,t,y,s}^{\text{u}}$$

$$+ \sum_{j \in \mathcal{S}_{j:n}} P_{jm,t,y,s}^{\text{j,inj}} - \sum_{j \in \mathcal{S}_{j:n}} P_{jm,t,y,s}^{\text{j,abs}} = 0$$

$$(: \lambda_{m,t,y,s})$$

Here,  $\mathcal{N}_m^{\text{AC}} := \{n \in \mathcal{N}^{\text{AC}} : mn \in \mathcal{E}^{\text{AC}}\}$  and  $\mathcal{N}_m^{\text{DC}} := \{e \in \mathcal{N}^{\text{DC}} : me \in \mathcal{E}^{\text{AC-DC}}\}$  respectively denote the AC and DC neighbors of  $m \in \mathcal{N}$ . On the DC network side the nodal power balance equation is non complicating:

$$\sum_{m \in \mathcal{N}_e^{\text{AC}}} P_{em,t,y,s}^{\zeta,\text{DC}} + \sum_{f \in \mathcal{N}_e^{\text{DC}}} \sum_{l \in \mathcal{S}_{\ell:\{ef\}}^{\text{DC}}} P_{l:ef,t,y,s}^{\ell} = 0. \quad (21)$$

$$e \in \mathcal{N}^{\text{DC}}, \quad t \in \mathcal{S}_t, \quad y \in \mathcal{S}_y, \quad s \in \mathcal{S}_s.$$

### B. Zonal Market Model

To model a zonal market we start by partitioning the network nodes into a set  $\mathcal{Z}$  of disjoint market zones, so that  $\mathcal{N} = \bigcup_{z \in \mathcal{Z}} z$ . The edges are also partitioned into inter-zonal edges  $\mathcal{E}^{\text{te}} \subseteq \{mn : m \in z, n \notin z, z \in \mathcal{Z}\}$  and intra-zonal edges  $\mathcal{E}^{\text{br}} \subseteq \{mn : m \in z, n \in z, z \in \mathcal{Z}\}$ . For ease of notation, the optimization variables for transmission lines along these edges are denoted as  $(\theta^{\text{te}}, \alpha^{\ell,\text{te}})$  and  $(\theta^{\text{br}}, \alpha^{\ell,\text{br}})$ , respectively. The superscripts refer to two new agents we will introduce, the Transmission Expansion agent ( $\mathcal{A}^{\text{te}}$ ) and the Balancing Responsible agent ( $\mathcal{A}^{\text{br}}$ ). We re-group the optimization variables into agents  $\mathcal{A}^{\text{te}}$  and  $\mathcal{A}^{\text{br}}$  as follows:

$$\mathcal{A}^{\text{te}} = (\mathcal{A}_w, \mathcal{A}_j, \mathcal{A}_e, \mathcal{A}_o^{\text{te}}) \quad \text{and} \quad \mathcal{A}^{\text{br}} = (\mathcal{A}_w, \mathcal{A}_j, \mathcal{A}_e, \mathcal{A}_o^{\text{br}}),$$

where  $\mathcal{A}_o^{\text{te}}$  differs from  $\mathcal{A}_o$  in that the transmission lines considered are restricted to inter-zonal connections.  $\mathcal{A}_o^{\text{br}}$  is the complement considering only intra-zonal connections. Furthermore, we define zonal power balance equations for both the AC and DC networks as in (22) and (23).

$$\left. \begin{aligned} & \sum_{m \in z} \left( \sum_{e \in \mathcal{N}_m^{\text{AC}}} P_{me,t,y,s}^{\zeta,\text{AC}} - \sum_{g \in \mathcal{S}_{g:n}} P_{g:m,t,y,s}^g \right. \\ & + \sum_{n \in \mathcal{N}_m^{\text{AC}}} \sum_{l \in \mathcal{S}_{\ell:\{mn\}}^{\text{te,AC}}} P_{l:mn,t,y,s}^{\ell} - \sum_{u \in \mathcal{S}_{u:n}} P_{u:m,t,y,s}^u \\ & \left. + \sum_{j \in \mathcal{S}_{j:n}} P_{j:m,t,y,s}^{\text{j,inj}} - \sum_{j \in \mathcal{S}_{j:n}} P_{j:m,t,y,s}^{\text{j,abs}} \right) = 0 \end{aligned} \right\} \begin{aligned} & z \in \mathcal{Z}, \\ & t \in \mathcal{S}_t, \\ & y \in \mathcal{S}_y, \\ & s \in \mathcal{S}_s, \\ & (: \lambda_{z,t,y,s}^z) \end{aligned} \quad (22)$$

$$\sum_{e \in z} \left( \sum_{m \in \mathcal{N}_e^{\text{AC}}} P_{em,t,y,s}^{\zeta,\text{DC}} + \sum_{f \in \mathcal{N}_e^{\text{DC}}} \sum_{l \in \mathcal{S}_{\ell:\{ef\}}^{\text{te,DC}}} P_{l:ef,t,y,s}^{\ell} \right) = 0$$

$$z \in \mathcal{Z}, \quad t \in \mathcal{S}_t, \quad y \in \mathcal{S}_y, \quad s \in \mathcal{S}_s \quad (23)$$

In a zonal market, (22) provides the market clearing condition. The dual variable of the constraint is the marginal price of energy at all nodes within zone  $z$ . As all nodes in a single market zone have a common energy price, the price signals of congestion are suppressed. This further complicates the already difficult problem of GATE. To overcome this difficulty a multi-level approach is adopted, whereby expansion planning is achieved via a four-step solution method. This solution method is presented in Fig. 2.

**Step one** is to calculate the inter-zonal network expansion by determining the location and capacity of transmission lines between market zones under the assumption of zero intra-zonal

congestion. Specifically, the state of binary investment decision variables  $\alpha^{\ell,\text{te}}$  are determined. Mathematically, this is accomplished by solving (24) ((5) with (24a) substituted for (2a)) subject to constraints (6) through (19) and the zonal power balance constraints (22) and (23). The resulting  $\alpha^{\ell,\text{te}}$  variables are passed to step two as parameters where intra-zonal transmission and generation expansion is performed.

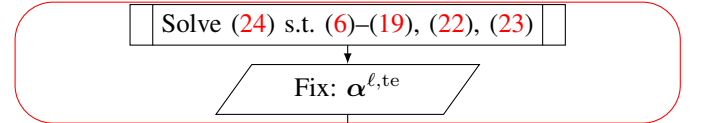
$$\max_{\mathcal{A}^{\text{te}}} \mathcal{U} := \sum_{s \in \mathcal{S}_s} \pi_s \sum_{y \in \mathcal{S}_y} f_y^H \sum_{t \in \mathcal{S}_t} [(4a) + (4b)] - f_y^Y [(1a) + (2b) + (3a) + (24a)] \quad (24)$$

$$\sum_{\{mn\} \subseteq \mathcal{N}} \sum_{\tilde{l} \in \tilde{\mathcal{S}}_{\ell:\{mn\}}} \alpha_{l:\{mn\},y}^{\ell,\text{te}} \cdot I_{\tilde{l},y} \quad (24a)$$

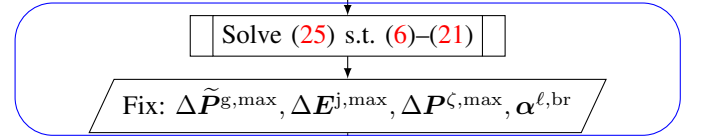
**Step two** determines intra-zonal expansion while respecting the inter-zonal capacity limitations determined in step one ( $\alpha^{\ell,\text{te}}$ ) as well as nodal power balance. To achieve nodal balance at the lowest cost, intra-zonal congestion can be eliminated via the construction of new lines ( $\alpha^{\ell,\text{br}}$ ), the expansion or reduction of newly added OWPPs and/or storage ( $\tilde{P}_g^{\text{g,max}}, E_j^{\text{j,max}}$ ) or the curtailment and/or re-dispatch of network generators ( $\mathcal{S}_g$ ). Mathematically, this is accomplished by solving objective (25) ((5) with (25a) substituted for (2a)) subject to nodal power balance (20) and (21) as well as the remaining network constraints (6) – (19).

$$\max_{\mathcal{A}^{\text{br}}} \mathcal{U} := \sum_{s \in \mathcal{S}_s} \pi_s \sum_{y \in \mathcal{S}_y} f_y^H \sum_{t \in \mathcal{S}_t} [(4a) + (4b)] - f_y^Y [(1a) + (2b) + (3a) + (25a)] \quad (25)$$

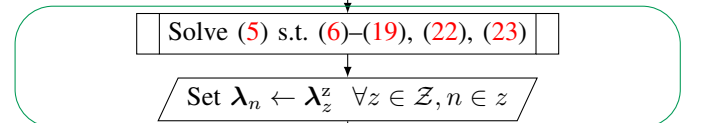
#### Find Inter-Zonal Network



#### Find Intra-Zonal Network



#### Forecast Power Flows



#### Correct Nodal Imbalance

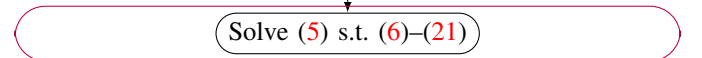


Figure 2: Flowchart of solution method for zonal market clearing formulation. “Solve” refers to the specified equations considering any fixed decision variables determined in an earlier step.

$$\sum_{\substack{\{mn\} \subseteq \mathcal{N} \\ mn \in \mathcal{E}^{br}}} \sum_{\tilde{l} \in \tilde{S}_{\ell:\{mn\}}} \alpha_{\tilde{l}:\{mn\},y}^{\ell,br} \cdot I_{\tilde{l}:\{mn\},y} \quad (25a)$$

**Step three** is performed post network expansion, i.e., all investment decision variables are fixed. A power auction is held considering only inter-zonal capacity constraints. This step simulates the day-ahead spot market and provides the forecast of inter-zonal power flows and the zonal market clearing prices based on an optimal dispatch. In the case of congestion free power flows this is the final step. When congestion is present, the additional step of re-dispatch is needed to relieve congestion and balance the network.

**Step four:** re-dispatch. The final cost of a zonally cleared energy market depends on the re-dispatching mechanism chosen. In the EU both market and regulatory based re-dispatch exist [36]. In this work we have chosen an idealized RDCC and argue that this represents an upper bound on possible zonal market benefits. Our argument is as follows.

In RDCC, an all knowing balancing authority calls on the lowest cost available generation and/or load to up or down regulate during re-balancing actions. Generators required to up regulate are compensated at their marginal price, while those required to down regulate are permitted to keep profits made from the spot market but must return any avoided variable costs (e.g. unused fuel costs). Since participants in RDCC are contractually obliged to participate at their marginal rates and we are assuming perfect transparency from generators regarding their marginal cost and available capacity, a market based re-dispatch could only, at best, achieve an identical re-dispatch cost.

Of course, in practice, the assumption of perfect transparency by market participants is unrealistic as this requires the sharing of private information. As such, we are not arguing RDCC is better than a market based re-dispatch mechanism. Rather, that in its idealized form it describes the upper bound on efficient re-dispatch.

Together, steps one through four describe the approach used for GATE planning in zonal markets. Alone, steps three and four describe an energy auction which can be run on any topology previously determined. For example, a topology determined using the nodal market approach described in section III-A can be operated within a zonal market structure.

## IV. TEST CASE

### A. Domain

A test grid ( $\mathcal{G}$ ) in the North Sea is modelled. The onshore and offshore nodes considered are displayed in Fig. 3 and their coordinates listed in table V of the appendix. The grid is inspired by the proposed TYNDP projects summarized in table VI of the appendix [6]. It is not the intention of this study to investigate the feasibility of these projects in detail, but rather to anchor the test grid within a practically and politically feasible space.

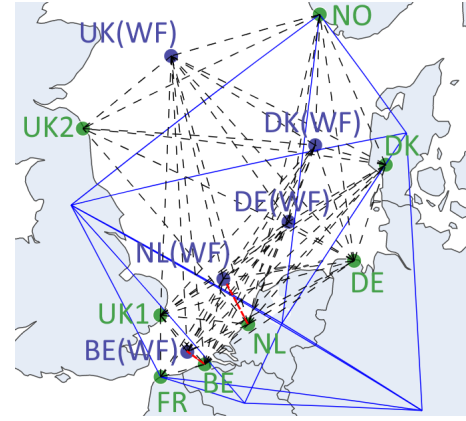


Figure 3: North Sea domain. Lines: NTCs (solid blue), HVDC (dashed black), HVAC (dashed red).

Table I: Infrastructure costs (excluding cables) [41], [42].

Component	OWPPs	Onshore converters	Offshore converters	Onshore storage	Offshore storage
Cost	2100	192.5	577.5	183	275

\*Costs are in €/kW and €/kWh (storage)

### B. Candidate Expansion

Candidate generation, transmission and storage assets can be expanded at a cost specified in table I. The maximum allowable capacity for OWPPs ( $P_{g,\max}$ ), HVDC converters ( $P_{\zeta,\max}$ ) and storage ( $E_{j,\max}$ ) are listed in table V of the appendix. At onshore nodes a dimensioning incident of  $\pm 3$  GW is assumed, hence onshore converters are limited to 3 GW while offshore converters can reach sizes of 4 GW. Storage is assumed to be a four-hour duration, lithium ion system. Candidate connections for HVAC and HVDC are shown in Fig. 3. The details of the candidate cable types and their costs are summarized in table VII of the appendix.

### C. Existing Generation

The existing energy mix ( $\bar{P}^g$ ) in each country is sourced from the ENTSO-E TYNDP, which provides a baseline as well as futures scenarios for the energy mix of European countries. The projected scenarios are for years 2030 and 2040 [43], [6]. Further details are provided below. Assumptions for marginal costs of generating sources are listed in table VIII of the appendix.

### D. Onshore grid

The onshore grid is modelled as existing transmission lines with maximum capacities equal to the Net Transfer Capacities (NTCs) specified in table IX of the appendix. These lines are displayed in blue in Fig. 3. The onshore NTCs remain static through the simulation years.

### E. Demand

Hourly demand data ( $P^u$ ) is taken from the TYNDP. Meeting demand at all times is ideal. When this is not possible, however, load defined as Demand Side Response (DSR) can

be shed at a cost 119 €/MWh. In the event that further load must be shed, the Value Of Lost Load (VOLL) is 5 k€/MWh. DSR does affect market price formation while load shedding does not. During times of extreme energy scarcity such as load shedding events an energy price cap of 180 €/MWh is enforced based on EU regulation 2022/1854 [44]. GCS is calculated based on a constant consumer bid price of 150 €/MWh.

### F. Scenarios

In the TYNDP, projections are made for future generation and demand via scenarios that consider different paths towards a net zero 2050. In this study the National Trends (NT), Distributed Generation (DG) and Global Ambition (GA) scenarios are included. In brief, NT is based on the National Energy Climate Policies, DG assumes mass societal adoption of distributed RES and GA considers a global movement towards the targets of the Paris Agreement. Pairing historical RES generation time series ( $\Psi^g$ ) from years 2014 and 2015 results in six scenarios in  $\mathcal{S}_s$ . Each are considered to have an equally likely probability of occurrence  $\pi_s$ .

Due to computational requirements each simulation year is clustered into four 24-hour days. The simulation years are 2020, 2030 and 2040. The representative days are found via the  $k$ -medoids clustering method [45]. The temporal correlation between the various time series is maintained. Ten calendar years per simulation year are considered: 2020-2029 is modelled with 2020 data, 2030-2039 with 2030 data and 2040-2049 with 2040 data. For full details on the methodology behind the scenario generation including aspects such as how resource adequacy is ensured we refer the reader to the TYNDP [6].

## V. RESULTS

The presented methodology is applied to  $\mathcal{G}$  to compare the effects of an nOBZ, zOBZ and an HMD considering multiple OWPPs. The market structure case studies are as follows:

- Each OWPP is part of its home market zone (HMD).
- All OWPPs form a common offshore market (zOBZ).
- Each node is its own market zone (nOBZ).

The resulting topologies are displayed in Fig. 4 through 6. The figures present the selected transmission lines and their capacities as well as the build schedule. The same information is provided for the OWPPs, HVDC converters and storage in table II. In all topologies, HOAs are dominant features. Only in the HMD and only for the closest wind development region to shore (Belgium) is a radial connection selected.

A breakdown of transmission, OWPP and storage developer costs and benefits are provided in table III. The net benefits, GCS and re-dispatch costs of each topology are ranked by social welfare in table IV.

There is little difference between the social welfare obtained under all variations of the nodal market structure (nOBZ, HMD\* and zOBZ\*). Three different topologies, all with similar levels of social welfare and a global lower bound (nOBZ), effectively demonstrate the flatness of the solution space and hence the limited value attached to the certificate of optimality. Planners should therefore not be overly concerned about

Table II: Expansion planning schedule of grid  $\mathcal{G}$ .

Year	nOBZ			HMD			zOBZ		
	'20	'30	'40	'20	'30	'40	'20	'30	'40
	$P_{ne,y}^{C,\max}$ [GW]								
UK1	2.9	3	3	3	3	3	2.4	3	3
FR	2.4	2.4	3	2.4	2.4	2.4	2.4	3	3
BE	0	0	1.8	0	0	2.4	0	0.6	1.5
NL	2.4	2.4	3	2.4	3	3	2.4	2.4	2.4
DE	2.4	2.4	3	3	3	3	2.4	2.4	3
DK	1.6	2.4	2.4	1.7	1.9	1.9	0	2.4	2.4
NO	3	3	3	3	3	3	3	3	3
UK2	1.9	2.4	3	1.7	2.4	2.4	0	3	3
BE(WF)	0.5	0.6	0.6	0	0	0	0	0	0
DE(WF)	3.7	3.7	3.7	3.7	3.7	3.7	3.6	3.7	3.7
NL(WF)	3.8	3.8	3.8	3.8	3.8	3.8	3.8	3.8	3.8
DK(WF)	3.7	3.7	3.8	3.7	3.7	3.8	3.7	3.7	3.8
UK(WF)	3.2	3.4	3.6	3.2	3.4	3.6	2.4	3.4	3.6

OWPPs: All 4 GW in 2020 (nOBZ, HMD).

All 4 GW in 2020 except UK(WF) is 3.9 GW in 2020, then expanded to 4 GW in 2030 (zOBZ).

Storage: 1 GWh of storage is scheduled in Holland in 2040 (nOBZ, HMD, zOBZ).

Table III: Summary of lifetime costs and benefits for  $\mathcal{G}$  in B€.

	Transmission		OWPP		Storage	
	Cost	Benefits	Cost	Benefits	Cost	Benefits
nOBZ	21.754	64.147	42.000	134.135	0.059	0.058
HMD*	22.380	64.722	42.000	133.700	0.059	0.058
zOBZ*	22.984	70.453	41.885	125.568	0.059	0.057
nOBZ**	22.984	57.703	41.885	135.241	0.059	0.056
nOBZ*	21.754	53.452	42.000	139.866	0.059	0.057
nOBZ*	21.754	49.015	42.000	143.459	0.059	0.047
HMD	22.380	48.526	42.000	144.152	0.059	0.046

HMD\*: The HMD topology operating in an nOBZ market.

zOBZ\*: The zOBZ topology operating in an nOBZ market.

nOBZ\*: The nOBZ topology operating in an HMD market.

nOBZ\*\*: The nOBZ topology operating in a zOBZ market.

Table IV: Summary of lifetime Social Welfare for  $\mathcal{G}$  in B€.

	Net Benefit	GCS	Re-dispatch	Social Welfare	Difference [%]
nOBZ	134.527	1920.331	0.000	2054.858	-
HMD*	134.040	1920.299	0.000	2054.340	-0.03
zOBZ*	131.151	1922.617	0.000	2053.767	-0.05
zOBZ	128.073	1926.606	128.596	1926.083	-6.27
nOBZ**	129.561	1921.987	127.006	1924.543	-6.34
nOBZ*	128.707	1924.729	145.615	1907.821	-7.16
HMD	128.284	1916.556	155.168	1889.672	-8.04

\*-entries in the first column are as in table III.

The last column is the change in social welfare compared to the nOBZ.

developing a uniquely optimal configuration as the problem's uncertainty dwarfs the difference between a good solution and the best solution.

The benefit of using a nodal based pricing mechanism is clearly demonstrated. All zonal pricing models result in a decrease in social welfare of 6-8% compared to nodal pricing. The worst performing market structure is the HMD. It seems, knowing the market structure a priori is not essential from a planning perspective as each design operates relatively well under a changing market design.

Despite the poor performance of the zonal market models in the zonal markets for which they were intended, the high quality of their nodal market variations suggests merit from a decomposition perspective. The computation times obtained on an intel core-7 1.9 GHz processor with 16 GB of RAM are:

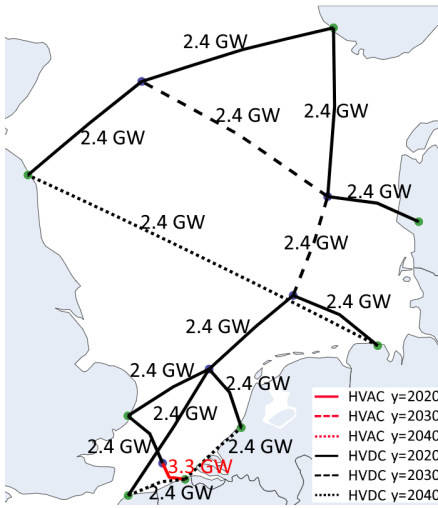


Figure 4: nOBZ  $\mathcal{G}$  topology.

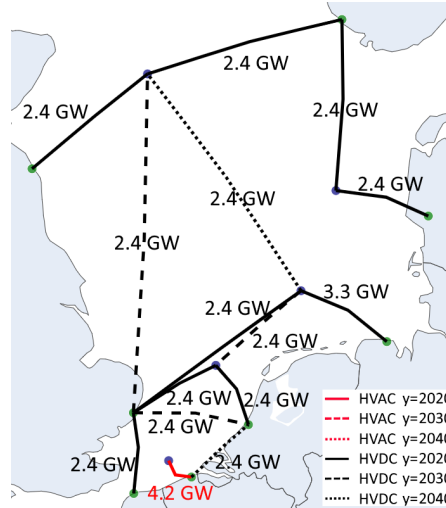


Figure 5: HMD  $\mathcal{G}$  topology.

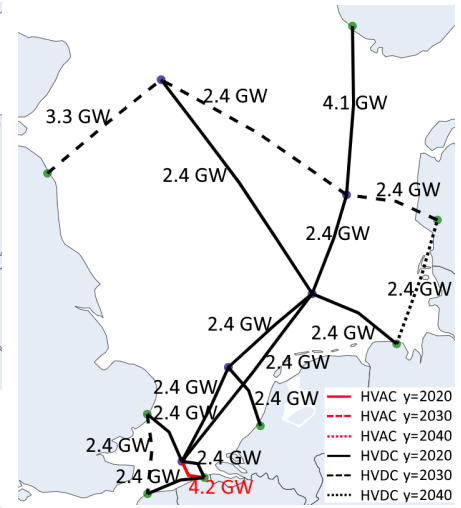


Figure 6: zOBZ  $\mathcal{G}$  topology.

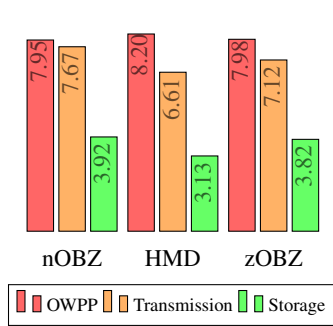


Figure 7: Yearly percent return on investment for  $\mathcal{G}$ .

zOBZ/HMD:  $\approx 2.5$  hours, the nOBZ: halted after twelve hours with a small optimality gap of 0.04% remaining. Zonal models scale better than nodal due to the natural decomposition along intra and inter zonal lines.

The three nodal market models may have little variation in social welfare but do have variation in how agent benefits are distributed. For example, nOBZ results in 6.8% higher benefits for an OWPP developer than in zOBZ\*. There is no free lunch of course as this is at the expense of the transmission developer which sees a decrease in benefits of 9%. The ability to adjust the distribution of benefits among stakeholders without sacrificing overall social welfare may prove useful.

All market mechanisms result in a positive return on investment for all agents (Fig. 7). The highest return for transmission and storage developers occurs under an nOBZ while OWPP developers do best in an HMD. By examining the average energy prices per node in Figs. 8 and 9 we see why. The HMD has the highest average energy prices both offshore and onshore. While this translates to higher profits for OWPP developers, it is bad for consumers and lowers the overall social welfare. In our model, the average European wide energy price for the HMD is 93.23 €/MWh, for the zOBZ it is 91.21 €/MWh and for the nOBZ it is 90.86 €/MWh.

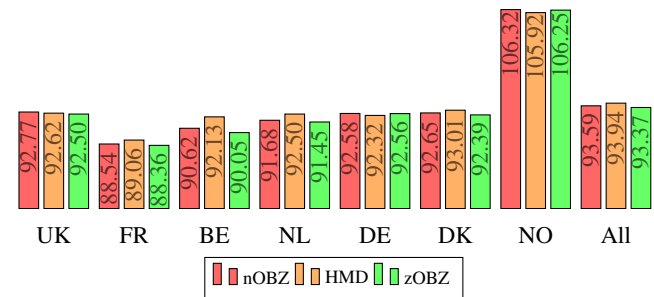


Figure 8: Average onshore energy prices for  $\mathcal{G}$  [€/MWh].

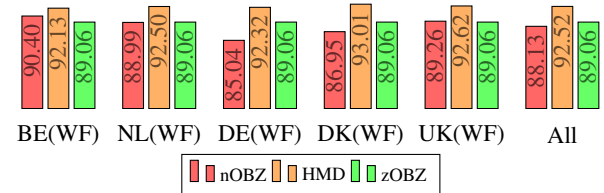


Figure 9: Average offshore energy prices for  $\mathcal{G}$  [€/MWh].

There is very little difference in wind curtailment between market designs, which amounts to essentially zero. This is shown in Fig. 10. Although the zOBZ results in about three times the curtailment compared to the nOBZ and the HMD, it is still only about 0.5% of the total energy production.

The cost to re-dispatch varies substantially between zonal market models. The highest re-dispatch costs are associated with HMDs and the lowest with zOBZs. A breakdown of the re-dispatch costs by generation type is presented in Fig. 11. It is interesting that in the home market designs load shedding makes up about 5% of the overall re-dispatch cost. It is not that more load is shed in this market structure, as load shedding is fairly constant at about 3.5 TWh across all market models (Fig. 10), but rather that the onshore-offshore congestion constraint is binding but not enforced. This is a variation on the pivotal supplier problem discussed in section II with the exception

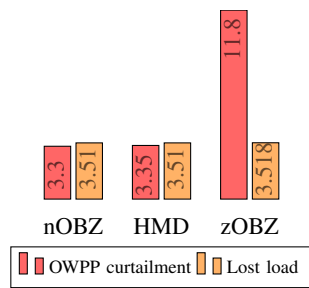


Figure 10: OWPP curtailment and lost load in TWh. Potential OWPP production: 2287 TWh (nOBZ/HMD), 2284 TWh (zOBZ). Total load: 50366 TWh.

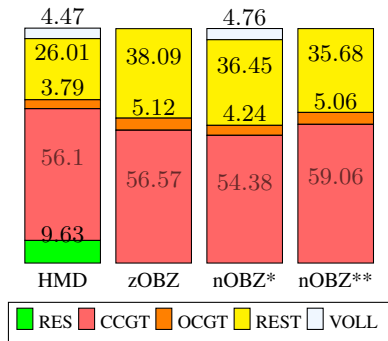


Figure 11: Percent breakdown of re-dispatch costs.

that VOLL does not affect the spot price formulation so the zOBZ and nOBZ\*\* see the energy price cap of 180 €/MWh rather than the 5k€/MWh for VOLL avoiding windfall profits for generators.

It is worth discussing the low level of storage selected in all topologies of our simulation. We have identified two potential reasons for this observation. Firstly and simply the cost of storage, as is specified in [41], may be too high. Alternatively, we suspect that the exclusion of certain factors, such as a two-level market, reserve market or unit commitment constraints (e.g. ramping rate, generation block size, start-up costs, or seasonality), may prevent adequately capturing the profitability for storage developers. This investigation is saved for future work.

## VI. CONCLUSION

This work presents a model for expansion planning in nodal and zonal market designs, aiming to maximize social welfare. A test case in the North Sea ( $\mathcal{G}$ ) is used to study the impact of market design on network topology optimization. From our simulation results some regulatory and modelling based observations can be made.

From the regulatory perspective, in our analysis, the nOBZ market structure results in maximum social welfare and the lowest European wide average energy prices. Additionally, in zonal market structures, the pivotal supplier effect should be considered to avoid artificially inflating the perceived social welfare. Market conditions were found to have a greater impact on social welfare than network topology, with all three topologies yielding comparable levels of social welfare in an

nOBZ. The expansion plan based on an nOBZ has a continuous upper bound on social welfare, suggesting a relatively flat solution space and providing flexibility in the distribution of benefits among stakeholders without sacrificing overall social welfare.

From the modelling perspective, a zonal planning approach has computational advantages over a nodal one and a topology developed assuming one market structure can operate well under a different market structure. This implies a zonal approach may prove a promising starting point for intractable problems under an nOBZ. Based on these observations we propose some recommendations moving forward. A clear regulatory structure for the offshore energy market is needed to allow developers to predict future revenues. Our results indicate this should be in the form of an nOBZ. Prior even to the development of clear market regulations, designers are wise to perform generation and transmission planning under the assumption that an nOBZ will be implemented as the obtained topologies will likely also perform well if a change of market design is required. When computational power is a constraint, a decomposition strategy based on a zonal market design appears to be beneficial.

Finally, the authors acknowledge limitations in this study and suggest future work to improve and extend the methodology. The scenario modelling of ENTSO-E does not consider projected NTC expansion between market zones, possibly resulting in an overestimation of congestion. Higher resolution data or NTCs modelled as optimization variables could address this. Modelling a two-stage market and better system flexibility through unit commitment constraints could improve the reliability of optimal storage expansion calculations, but may result in intractability or high computation times. A zonal decomposition approach is promising, but more efficient optimization strategies, such as fast consensus ADMM [46] or Bender's decomposition [47], should also be explored. Considering these limitations, the authors caution that the intent of this work is not to claim an optimal expansion plan has been developed. This paper is not investment advice. Rather the test case is presented with the intention of providing a practice discussion point regarding the overall conversation on market design in the North Sea.

## APPENDIX

Supplementary data describing the boundary conditions of the North Sea test case is provided in this section. This includes modelling coordinates (table V), relevant TYNDP projects (table VI), candidate cable data (table VII), marginal prices of generators (table VIII) and modelled onshore NTCs (table IX).

## REFERENCES

- [1] Open AI, "ChatGPT Large language model," 2023. [Online]. Available: <https://chat.openai.com/chat>
- [2] European Commission, "Re power EU with clean energy," 2022.
- [3] D. Jorgensen, T. Van der Straeten, R. Jetten, and R. Habeck, "The declaration of energy ministers on the North Sea as a green power plant of Europe," 2022.
- [4] "The Paris Agreement," united Nations Treaty Collection XXVII 7.d.

Table V: Location of nodes in test grids and maximum capacity of candidate converters, storage and OWPPs.

Point	Longitude	Latitude	$\widehat{P}_{\zeta}^{mx}$	$\widehat{P}_{gw}^{mx}$	$\widehat{E}_j^{mx}$
UK-1	52.2102517	1.5737432	3 GW	-	1 GW
BE-2	51.3208101	3.2076794	3 GW	-	1 GW
DE-3	53.6704307	7.8461971	3 GW	-	1 GW
DK-4	55.6142004	8.728994	3 GW	-	1 GW
BE-5	51.5350934	2.5964400	4 GW	2 GW	20MW
DE-6	54.346105	5.5239962	4 GW	4 GW	20MW
DK-7	55.9011491	6.2224031	4 GW	4 GW	20MW

Table VI: North Sea TYNDP projects inspiring test grids

Project	Type	Location	ref.
NeuConnect	HVDC Inter-connector	DE, UK	[48]
Nautilus	HVDC Inter-connector	BE, UK	[49]
Triton Link	HVDC Inter-connector	BE, DK	[50]
Aminth Energy	HVDC Inter-connector	DK, UK	[51]
North Sea Wind Power Hub	OWPP	DE, DK, NL	[52]
N9.1, N9.2	OWPP	DE	[53]
MOG II	OWPP	BE	[54]

- [5] R. O'Sullivan, "Offshore wind in Europe key trends and statistics 2020," Wind Europe, Tech. Rep., 2021.
- [6] "ENTSOE TYNDP Ten year network development plan," accessed: 2022-05-17. [Online]. Available: <https://2022.entsoe-tyndp-scenarios.eu/>
- [7] European Commission, "Regulation (eu) 2022/869 of the european parliament and of the council of 30 may 2022," *Official Journal of the European Union*, 2022.
- [8] D. Van Hertem and M. Ghandhari, "Multi-terminal VSC HVDC for the European supergrid: Obstacles," *Renewable and sustainable energy reviews*, vol. 14, no. 9, pp. 3156–3163, 2010.
- [9] J. De Decker and A. Woyte, "Review of the various proposals for the European offshore grid," *Renewable energy*, vol. 49, pp. 58–62, 2013.
- [10] T. K. Vrana and O. B. Fosso, "Technical aspects of the North Sea super grid," *CIGRE Electra*, nov 2011.
- [11] J.-B. Curis, J. Descloux, N. Grisey et al., *Deliverable 1.3: Synthesis of available studies on offshore meshed HVDC grids*. PROMOTION-Progress on Meshed HVDC Offshore Transmission Networks, 2016.
- [12] E. Pierri, O. Binder, N. G. Hemdan, and M. Kurrat, "Challenges and opportunities for a European HVDC grid," *Renewable and Sustainable Energy Reviews*, vol. 70, pp. 427–456, 2017.
- [13] A. J. Conejo, L. Baringo, S. J. Kazempour, and A. S. Siddiqui, *Generation and Transmission Expansion Planning*. Cham: Springer International Publishing, 2016, pp. 115–167.
- [14] B. Stott, J. Jardim, and O. Alsac, "DC power flow revisited," *IEEE transactions on power systems*, vol. 24, no. 3, pp. 1290–1300, 2009.
- [15] J. A. Taylor and F. S. Hover, "Convex models of distribution system reconfiguration," *IEEE Transactions on Power Systems*, vol. 27, no. 3, pp. 1407–1413, 2012.
- [16] H. Ergun, J. Dave, D. Van Hertem, and F. Geth, "Optimal power flow for ACDC grids: Formulation, convex relaxation, linear approximation, and implementation," *IEEE Transactions on Power Systems*, vol. 34, no. 4, pp. 2980–2990, jul 2019.
- [17] J. Dave, H. Ergun, and D. Van Hertem, "Relaxations and approximations of HVDC grid TNEP problem," *Electric power systems research*, vol. 192, p. 106683, 2021.
- [18] L. Baringo and A. J. Conejo, "Transmission and wind power investment," *IEEE transactions on power systems*, vol. 27, no. 2, pp. 885–893, 2012.
- [19] Y. Zhou, L. Wang, and J. D. McCalley, "Designing effective and efficient incentive policies for renewable energy in generation expansion planning," *Applied Energy*, vol. 88, no. 6, pp. 2201–2209, 2011.
- [20] A. Chuang, F. Wu, and P. Varaiya, "A game-theoretic model for generation expansion planning: problem formulation and numerical comparisons," *IEEE Transactions on Power Systems*, vol. 16, no. 4, pp. 885–891, 2001.
- [21] F. H. Murphy and Y. Smeers, "Generation capacity expansion in imperfectly competitive restructured electricity markets," *Operations research*, vol. 53, no. 4, pp. 646–661, 2005.
- [22] J. Wang, M. Shahidehpour, Z. Li, and A. Botterud, "Strategic genera-

Table VII: HVAC(DC) candidate cables [42], [55].

	n-cm <sup>2</sup>	from	to	MVA	km	Cost
AC1	12-16	BE	BE(WF)	4213	61	1520
AC2	11-10	BE	BE(WF)	3319	61	1065
AC3	8-10	BE	BE(WF)	2414	61	785
AC4	11-16	NL	NL(WF)	3236	146	3345
AC5	12-6.3	NL	NL(WF)	2479	146	2338
DC1	4-15	-	-	4085	-	3593
DC2	4-10	-	-	3288	-	3194
DC3	2-20	-	-	2407	-	2575
DC4	2-10	-	-	1644	-	2372

Specific HVAC cables are listed as capacity is dependent on length due to reactive power. HVAC cable costs are in M€. HVDC cable costs are in €/m

Table VIII: Marginal price of generators [43].

Generation Type	€/kWh
PV, Hydro	0.018
Onshore wind	0.025
Offshore wind	0.059
Other RES	0.060
Gas CCGT	0.089
Nuclear	0.110
DSR	0.119
Gas OCGT, Coal, Pump storage, P2G, Other non-RES	0.120
Light oil	0.140
Heavy oil, Shale oil	0.150

Table IX: NTCs between countries in GW [43].

	BE	FR	UK	NL	DE	NO	DK
BE		4.3	1	2.4	1		
FR	4.3		4		3		
UK	1	4		1	1.4	2.8	1.4
NL	2.4		1		5	0.7	0.7
DE	1	3	1.4	5			3.5
NO			2.8	0.7			1.64
DK			1.4	0.7	3.5	1.64	

\*The 1.4 GW DE-NO NTC is not included in the onshore grid.

- tion capacity expansion planning with incomplete information," *IEEE Transactions on Power Systems*, vol. 24, no. 2, pp. 1002–1010, 2009.
- [23] A. Botterud, M. Ilic, and I. Wangenstein, "Optimal investments in power generation under centralized and decentralized decision making," *IEEE Transactions on Power Systems*, vol. 20, no. 1, pp. 254–263, 2005.
- [24] J. Lopez, K. Ponnambalam, and V. Quintana, "Generation and transmission expansion under risk using stochastic programming," *IEEE transactions on power systems*, vol. 22, no. 3, pp. 1369–1378, 2007.
- [25] S. J. Kazempour, A. J. Conejo, and C. Ruiz, "Strategic generation investment using a complementarity approach," *IEEE Transactions on Power Systems*, vol. 26, no. 2, pp. 940–948, 2011.
- [26] S. J. Kazempour and A. J. Conejo, "Strategic generation investment under uncertainty via benders decomposition," *IEEE Transactions on Power Systems*, vol. 27, no. 1, pp. 424–432, 2012.
- [27] X. Zhang and A. J. Conejo, "Robust transmission expansion planning representing long- and short-term uncertainty," *IEEE Transactions on Power Systems*, vol. 33, no. 2, pp. 1329–1338, 2018.
- [28] R. A. Jabr, "Robust transmission network expansion planning with uncertain renewable generation and loads," *IEEE Transactions on Power Systems*, vol. 28, no. 4, pp. 4558–4567, 2013.
- [29] B. Chen, J. Wang, L. Wang, Y. He, and Z. Wang, "Robust optimization for transmission expansion planning: Minimax cost vs. minimax regret," *IEEE Transactions on Power Systems*, vol. 29, no. 6, pp. 3069–3077, 2014.
- [30] V. Grimm, A. Martin, M. Schmidt, M. Weibelzahl, and G. Zöttl, "Transmission and generation investment in electricity markets: The effects of market splitting and network fee regimes," *European journal of operational research*, vol. 254, no. 2, pp. 493–509, 2016.
- [31] L. P. Garces, A. J. Conejo, R. Garcia-Bertrand, and R. Romero, "A bilevel approach to transmission expansion planning within a market environment," *IEEE Transactions on Power Systems*, vol. 24, no. 3, pp. 1513–1522, 2009.

- [32] “ENTSO-E position on offshore development market and regulatory issues,” 2020.
- [33] D. Schönheit, M. Kenis, L. Lorenz, D. Möst, E. Delarue, and K. Bruninx, “Toward a fundamental understanding of flow-based market coupling for cross-border electricity trading,” *Advances in Applied Energy*, vol. 2, p. 100027, 2021.
- [34] European Commission and Directorate-General for Energy, *Market arrangements for offshore hybrid projects in the North Sea*. Publications Office, 2020.
- [35] A. Moser, N. Bracht, and A. Maaz, “Simulating electricity market bidding and price caps in the European power markets s18 report,” European Commission and Directorate-General for Energy, Tech. Rep., 2017.
- [36] L. Hirth and I. Schlecht, “Market-based redispatch in zonal electricity markets,” *IO: Empirical Studies of Firms & Markets eJournal*, 2018.
- [37] H. Ergun, I. B. Sperstad, B. Espen Flo *et al.*, “Probabilistic optimization of t&d systems planning with high grid flexibility and its scalability,” KU Leuven, Tech. Rep., 2021.
- [38] L. Gurobi Optimization, “Gurobi optimizer reference manual,” 2020. [Online]. Available: <http://www.gurobi.com>
- [39] J. Bezanson, A. Edelman, S. Karpinski, and V. B. Shah, “Julia: A fresh approach to numerical computing,” *SIAM review*, vol. 59, no. 1, pp. 65–98, 2017.
- [40] J. Dave, H. Ergun, T. An, J. Lu, and D. Van Hertem, “TNep of meshed HVDC grids: ‘AC’, DC and convex formulations,” *IET Generation, Transmission and Distribution*, vol. 13, pp. 5523–5532(9), dec 2019.
- [41] Wesley Cole, A. Will Frazier, and Chad Augustine, “Cost Projections for Utility-Scale Battery Storage: 2021 Update,” NREL National Renewable Energy Laboratory, Tech. Rep., 2021.
- [42] PROMOTioN Workpackage 1, “Cost data collection report,” KU Leuven, Tech. Rep., 2020, (Internal document).
- [43] ENTSO-E, “Data set: Tyndp 2020 scenario file.”
- [44] European Commission, “Council regulation EU 2022/1854 of 6 October 2022 on an emergency intervention to address high energy prices,” *Official Journal of the European Union*, 2022.
- [45] L. Kaufman and P. Rousseeuw, *Partitioning Around Medoids (Program PAM)*. John Wiley & Sons, Ltd, 1990, pp. 68–125.
- [46] A. Themelis, L. Stella, and P. Patrinos, “Douglas-Rachford splitting and ADMM for nonconvex optimization: Accelerated and Newton-type algorithms,” *Computational Optimization and Applications*, vol. 82, pp. 395–440, 2022.
- [47] L. Baringo and A. J. Conejo, “Wind power investment: A benders decomposition approach,” *IEEE Transactions on Power Systems*, vol. 27, no. 1, pp. 433–441, 2012.
- [48] ENTSO-E, “Project 309 - NeuConnect,” 2022. [Online]. Available: <https://tyndp2020-project-platform.azurewebsites.net/projectsheets/transmission/309>
- [49] Elia Group, “Nautilus Hybrid Interconnector,” 2022. [Online]. Available: <https://www.elia.be/en/infrastructure-and-projects/infrastructure-projects/nautilus>
- [50] —, “Triton Link Hybrid Interconnector,” 2022. [Online]. Available: <https://www.elia.be/en/news/press-releases/2021/11/20211123%5Fpreliminary-study-on-hybrid-interconnector>
- [51] ENTSO-E, “Project 1051 - Aminth Energy Ltd,” 2022. [Online]. Available: <https://tyndp2020-project-platform.azurewebsites.net/projectsheets/transmission/1051>
- [52] Elia Group, “Project 335 - North Sea Wind Power Hub,” 2022. [Online]. Available: <https://tyndp2020-project-platform.azurewebsites.net/projectsheets/transmission/335>
- [53] 4C Offshore, “Project N9.1,N9.2 - German wind development zone,” 2022. [Online]. Available: <https://map.4coffshore.com/offshorewind/>
- [54] Elia Group, “TR 120 - Belgian Modular Offshore Grid II (MOG II),” 2022. [Online]. Available: <https://tyndp2022-project-platform.azurewebsites.net/projectsheets/transmission/120>
- [55] ABB high voltage cable unit, “HVDC light cables, submarine and land power cables,” ABB, Tech. Rep., 2006.